

Root Cause Analysis of Premature Failure in Reheater Bend Tube of a 700 MW Thermal Power Plant

R. K. Kumar, D. Laxman Rao

Materials Technology Division, Central Power Research Institute, Bangalore

Abstract - The root cause for the premature failure of a reheater tube bend of a 700 MW supercritical boiler after 15000 hrs of service was investigated. The chemical composition, mechanical properties, and microstructural degradation have been studied both on the failed and virgin tube material. The mechanisms involved in the failure process have been identified and the methodology to be followed for preventing recurrence of the incidence has been brought out.

Keywords: Boiler tube, reheater, sensitization, carbide precipitation, austenitic steels

Introduction

The failure of boiler tubes in Indian thermal plants is widely experienced in many thermal plants leading to forced outage of the plant. The no. of forced outages due to the failure of key boiler tube components such as superheater, reheater and economizer during 2015 – 18 in the range of 1230 to 1347 (Central Electricity Authority, 2020) in a year. A total of 378 failures have been reported in the case of reheater tubes over the last three years. Advanced material schemes have been presently used for supercritical boilers to improve the service life of the boiler components exposed to higher service temperatures.

The superheater and reheater components in a thermal power plant experience high-temperature working conditions and are primarily made from austenitic stainless steel grades of 347H, 321, and 304H. Among different grades, AISI 347H grade material is widely used because of its excellent creep resistance, oxidation and corrosion resistance [2-6] However, these steels undergo vulnerable conditions such as stress corrosion cracking (SCC), intergranular corrosion (IGCC),

embrittlement, coarsening of carbides, formation of sigma phase etc. during service. The titanium and niobium (Nb) stabilized SS347 grade are being used to avoid sensitization. During the outages, the possibility of pitting corrosion is imminent due to the accumulation of stagnant oxygen-rich water inside the reheater panel tubes.

Several failure mechanisms have been reported for the austenitic-grade steel tubes [2,7-10]. However, reports on the failure in bend are not widely available [2,11]. Under high-temperature conditions of 500 to 800°C, the sensitization phenomenon occurs in austenitic steels due to the precipitation of carbides at the grain boundaries and the depletion of chromium in the grains.

A 700 MW supercritical boiler reheater tube has failed in service after a period of 15000 hrs. To identify the reasoning for the failure, detailed analysis of chemical, mechanical, and microstructural properties, Scanning Electron Microscopy and precipitate analysis using Energy Dispersive Spectroscopy (EDS) analysis etc. were carried out. The technical details of the boiler unit are given in Table 1.

Table 1: Details of the boiler unit

Unit Capacity	700 MW, Supercritical
Year of Commissioning	2016
No Hours of service	15000 Hrs
Material of Reheater Tube	SA213 TP347H
Working pressure and Steam Pressure Tube Temperature	63.8 KSC 596 °C
Flue gas temperature in the vicinity of failed tube	1044 °C
RH tube Thickness	3.99 mm
RH tube Outer Diameter	63.5 mm

The properties of the failed tube and the virgin tube of the same batch have been compared. Detailed experimental investigations included visual inspection, Dimensional measurements, Chemical compositional analysis, a Hardness profile at different locations, Mechanical properties evaluation, Microstructural studies using an Optical microscope, and precipitate analysis using EDS.

Visual Examination

The photograph of the failed RH tube location (Coil no. 28 with tubes 12 to 14) inside the boiler showing multiple failures is shown in Fig. 1a. A total of 50 reheater tube coils were available inside the boiler. The analysis was carried out on the innermost bend loop tube which has shown radial cracking. The close-up view of the failed reheater tube showing a thin hairline longitudinal crack along the bend radius is shown in Fig. 1b. The longitudinal crack length was observed to be around 40 mm. The OD Side surface is covered with a black-coloured adherent scale. Spalling of the external scale in some areas was observed. Swelling or reduction in the wall thickness of the tube was observed near the crack opening. The cut cross sectional view of the tube confirmed the existence of the crack extending through the wall thickness (Fig. 1(b)).

Dimensional Measurement:

The thickness of the tube was measured on both ends as shown in Fig. 2, to account for erosion and swelling caused by any overheating issues. There was no discernible reduction in wall thickness both in the radial direction as well as the diametrically opposite region. The tube thickness was observed to be near to the design thickness value of 3.99 mm and the thickness readings were given in table -2. The dimension taken at the cross-section of the tube is shown in Fig. 3.

Table 2: Thickness readings at various locations

Distance from the one side of the tube(in mm)	Thickness(in mm)	
	90° of opening	180° of failed opening
0	3.73	4.06
20	3.71	4.05
40	3.69	4.09
60	3.66	4.08

80	3.67	4.11
100	3.69	4.12
120	3.72	4.09
140	3.72	4.11
160	3.73	4.13
180	3.77	4.13



Fig. 1(a) View of the Location of the failed tubes in the coils and 1(b) cross-sectional view of the ID side



Fig. 2 Wall thickness measurement locations along the bend tube

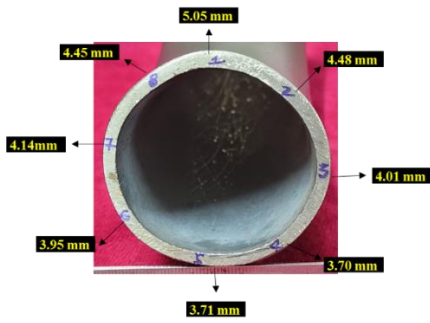


Fig. 3. Thickness measurements at the cracked end of the tube

Chemical Analysis

A ring piece of the failed tube end has been cut and analysed for chemical composition using an Optical Emission Spectrometer. The analysis was carried out on different regions of the tube, and the average results are given in Table 3. The observed results confirm that the RH tube metal is niobium-stabilized austenitic steel. The chemical composition of the reheater tube was found to be well within the specified range as per the ASTM standard A240/A240M-22a [12].

Table -3: Results of Chemical Composition Analysis

Composition, by weight %			
Elements	Failed Reheater Tube	Virgin tube	(Ref. Values of TP347H as per ASME)
C	0.063	0.057	0.04-0.10
Mn	1.423	1.59	< 2.00
Si	0.435	0.188	< 0.75
P	0.049	0.047	< 0.045
S	0.007	0.004	< 0.030
Cr	19.03	19.15	17.0-19.0
Ni	9.06	8.58	9.0-13.0
Nb	0.489	0.58	8 x %C to 1

Hardness

To ascertain the temperature-induced physical changes in the tube, the macro hardness in the Brinell scale was measured using portable Hardness tester equipment. The hardness values are given in Table 4. The measurements were taken along the length of the outer bend region (90° and 180 deg. opposite from the failed opening). The hardness on the cracked reheater tube has shown consistent values of around 120-170 BHN. The

hardness of the virgin tube has shown values in the range of 110 to 120 BHN

Table 4. Results of Hardness of Failed Tube

Measurement interval steps (mm)	Hardness, BHN	
	90° cracked region (Outer bend radii)	180° Opposite side of cracked opening
0	114	133
20	132	184
40	136	175
60	130	185
80	143	184
100	134	182
120	124	172
140	141	150
160	146	148

Mechanical Properties

A small section of tube metal was cut from a failed reheater tube and virgin tube, machined as per standard, and evaluated for its mechanical strength properties. Two samples were taken in the vicinity of the failed region, shown in Fig. 4. The load-displacement graph obtained for failed and new tubes is shown in Fig. 5. The yield strength, tensile strength, and elongation values were determined, and the results are given in Table 5.

Table 5. Results of Mechanical Properties

Tube description	Yield strength (MPa)	Ultimate strength (MPa)	Elongation (%)
Specimen ahead of thin line crack region	496	651	43.4
Specimen taken from	448	636	45.8
Virgin tube Sample-1	269	563	48.4
Virgin tube Sample-2	222	562	49.9
Ref. values as per ASME	≥205	≥515	≥ 40

Results indicated that the yield strength of the failed tube was nearly two times higher than that of the virgin tube. This appears due to the phenomenon of strain-induced precipitation hardening of the material. However, the ultimate tensile and elongation properties are well above the minimum requirements as per ASME standards.

Microstructural Examination

The metallurgical damage experienced by the tube was assessed at different locations in terms of their residual microstructure under an optical microscope as well as a Scanning Electron Microscope. Two samples were cut from the failed tube; one near the crack opening region and the other away from the crack region. The samples were prepared by polishing following standard metallographic practice. The finely polished sample was etched with Glyceregia etchant to reveal phases of grain boundaries and precipitates. The optical micrographs of the failed and

virgin tube samples are shown in Figs. 6 & 7. The microstructure of the Reheater tube revealed an austenitic structure with precipitated carbide phases along the grain boundary, typical of a sensitized structure. Sensitization of the grain boundaries with grain boundary thickening has been observed in the failed tube, typical of intergranular attack while the grain structure in the virgin tube was quite good. The precipitation of Chromium carbide ($Cr_{23}C_6$) was observed to have formed for service, indicating the fact that the tube has undergone temperature-induced phase transformation. The absence of corrosion species near the cracked edge is indicative that the material has not been subjected to stress corrosion cracking. Figures 6 & 7 show the microstructure of the failed tube at different locations and the virgin tube observed under different magnifications. The structure revealed a sensitized condition of the grain boundaries marked by the ditch structure.

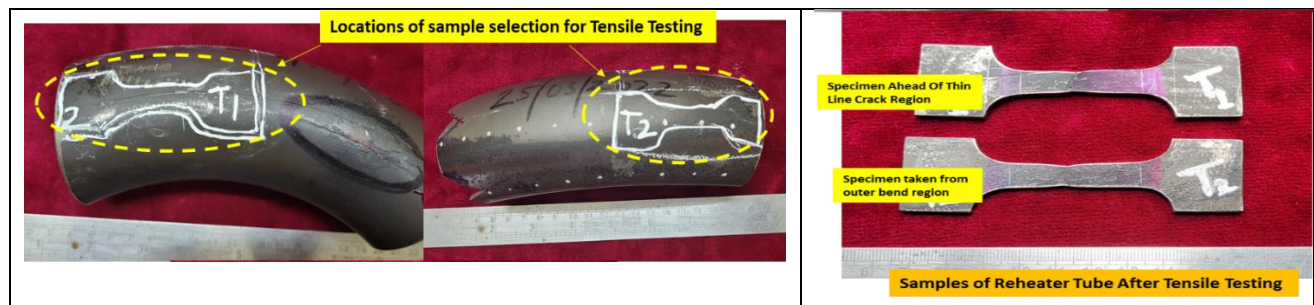


Fig. 4

Location of samples taken from the tube sample for tensile tests

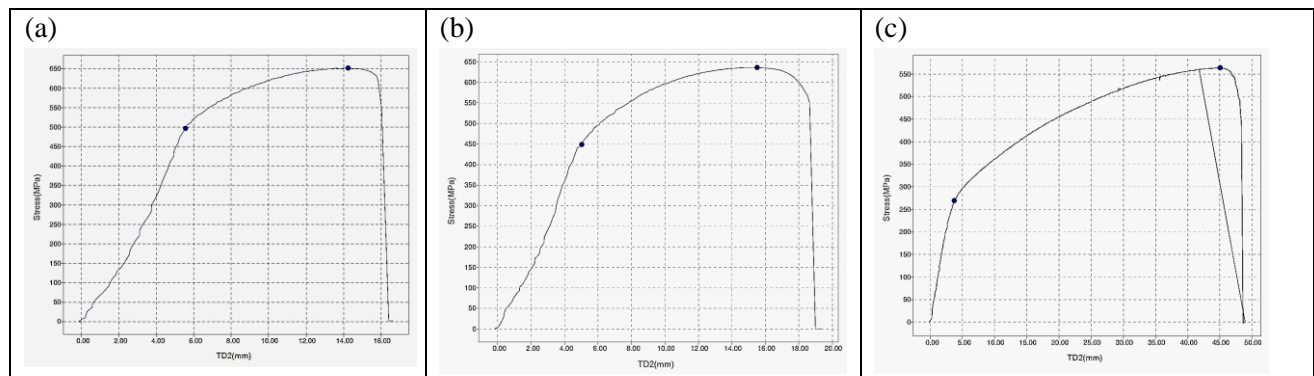


Fig. 5 Stress-Displacement Graph of the tensile sample taken at different regions, near thin hairline crack close to failure opening (a) outer bend region (b) virgin tube sample (c)

a)	b)	c)
----	----	----

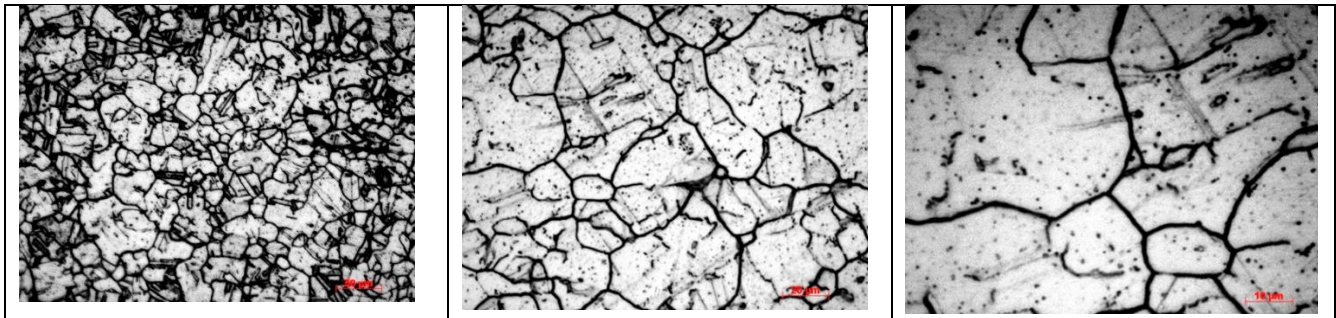


Fig. 6 Microstructure of the failed tube close to the cracked region at (a) 200x (b) 500x (c) 1000x.

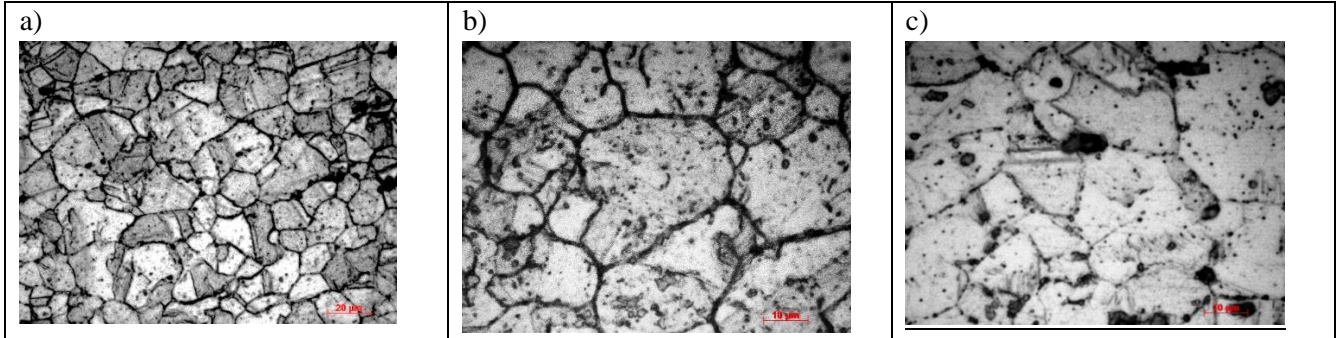


Fig. 7. Microstructure of the Failed RH tube near outer bend radius region (a) (b) revealing grain growth and sensitized structure and virgin tube micrograph (c)

SEM Micrographs & Precipitate Analysis by EDS.

The composition of the carbides precipitated along the grain boundary regions at various locations was analysed by EDS. The micrograph shows the concentration of stabilizing elements as observed on the grain regions and the chromium-rich carbides in the

grain boundaries are shown in Fig. 8 & 9. The SE micrographs of both cracked tubes showing the austenitic grain structure along with carbide precipitation along grain boundaries are shown in Fig. 10. Depletion of chromium, carbon and nickel was observed over the grain and the precipitate showed high chromium content.

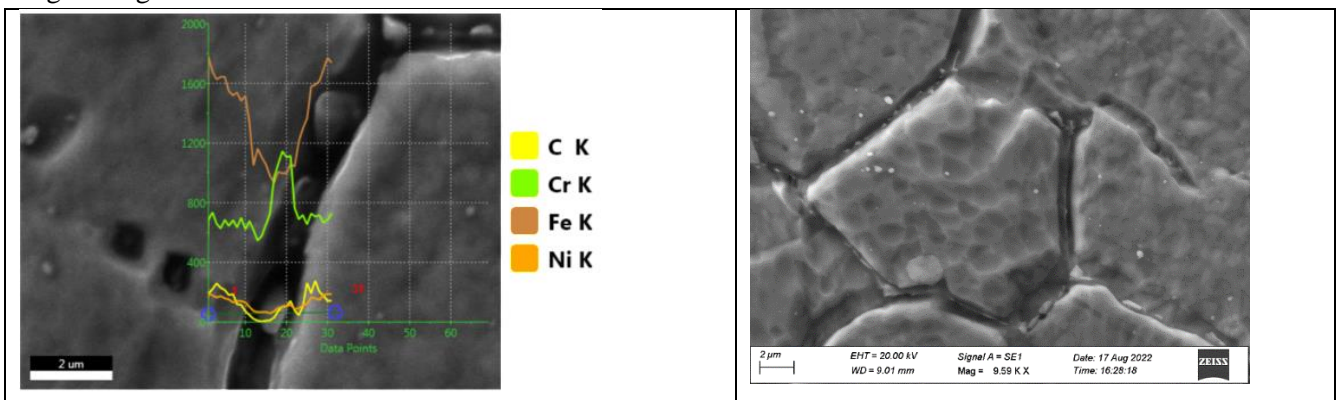


Fig. 8 Mapping of elemental concentration across grain and precipitate through Electron micrographs.

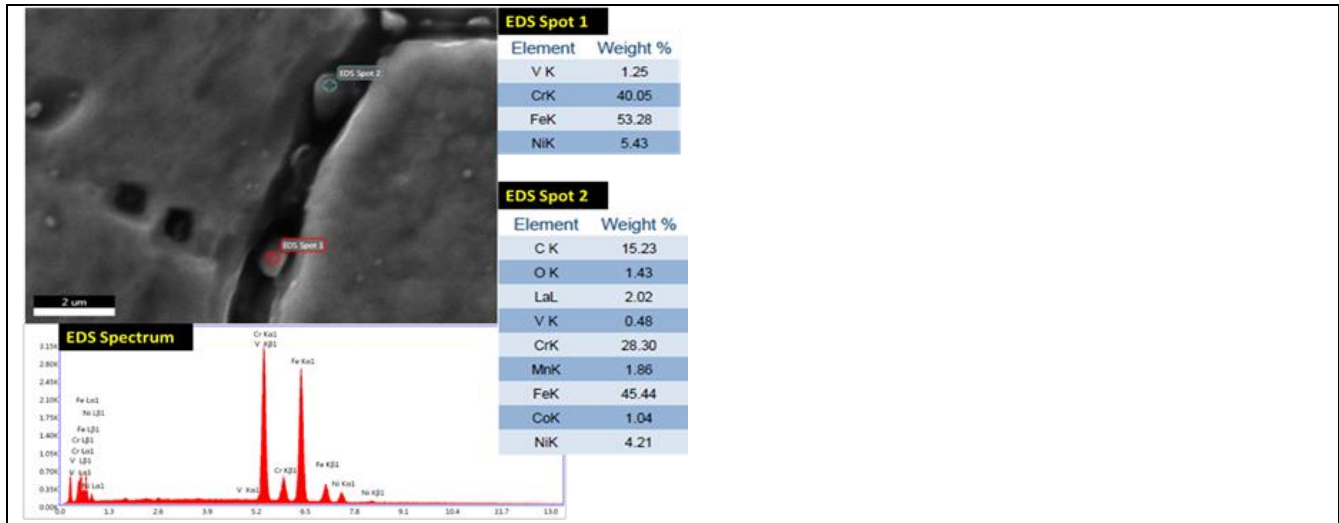


Fig. 9 EDS line scan spectrum along the grain boundaries confirming precipitation of chromium carbides - $Cr_{23}C_6$ along the grain boundary region

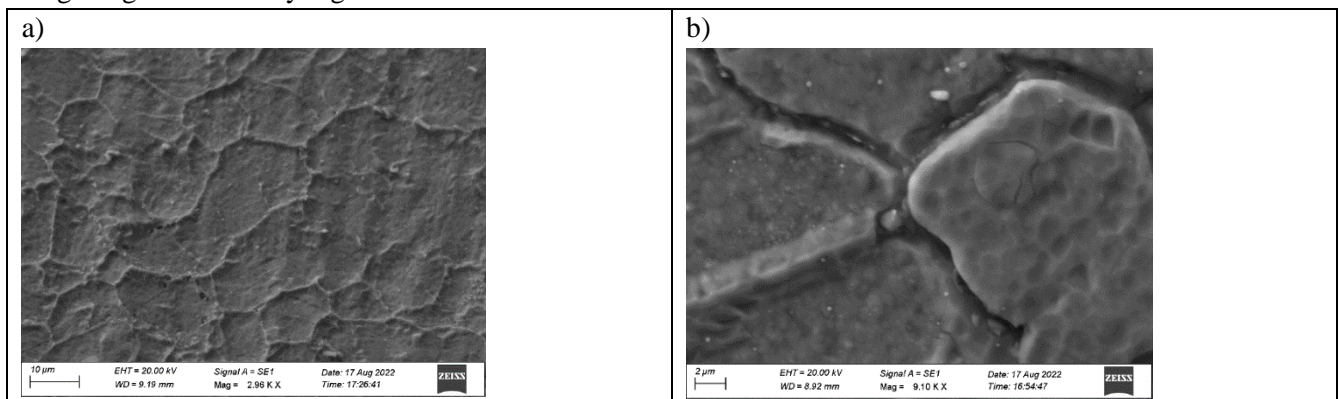


Fig. 10. Electron micrographs of Failed Reheater tube revealing austenitic grain structure (a) precipitation of carbides along the grain boundaries (b).

Results and Discussion

1. The chemical composition of the tube conforms to SA213 TP347H grade steel. However, the observed Nb/C ratio is observed to be lower than that of the minimum value of 10. The thickness measurements of the cross sections at both the ends of tube close to the cracked region have been shown to meet the design thickness value. However, the non-uniformity during the forming process during bending caused differential thickness across the section.
2. The Brinell hardness of the Reheater tube metal was observed to be around 120 to 170 BHN. The increase in hardness of the tube was observed up to 40% in the failed tube.
3. The microstructure of the tube close to the thin hairline crack region has shown a sensitized structure with chromium carbide precipitation along the grain

boundaries. The SEM analysis of the etched sample revealed large-sized precipitates concentrated along the grain boundaries & EDS analysis of those precipitates confirmed the presence of chromium carbides ($Cr_{23}C_6$).

4. The microstructure of the tube close to the thin hairline crack region has shown a sensitized structure with chromium carbide precipitation along the grain boundaries. The SEM analysis of the etched sample revealed large-sized precipitates concentrated along the grain boundaries & EDS analysis of those precipitates confirmed the presence of chromium carbides ($Cr_{23}C_6$).
5. While the yield strength and tensile strength of the failed reheater tube were found to be well within the minimum specified value as per ASME, the cracked tube has shown very high yield strength up to two times. The higher hardness and yield strength of the failed bend tube material are indicative of strain-induced precipitation hardening.

Conclusions

The U bend tube invariably undergoes a cold or warm forming process (plastic straining process) during the bending process which introduces severe stresses along the bend sections. The solution annealing treatment has been practised as a secondary process after forming/bending. The solution annealing at an appropriate temperature provides stress-relief conditions as well as a reduction in dislocation generated by the processing. The reported temperature range for solution annealing is 1040 to 1065 °C and the stabilization treatment is 900 to 920°C. Also, in the chemically stabilized austenitic steel, the solution annealing promotes the precipitation of niobium carbides (NbC) rather than chromium carbides as Nb has more affinity towards carbon than chromium. However, to maintain the precipitated NbC during the continued exposure to service temperatures of 510 to 700°C, the microstructure needs to be thermally stabilized. This is particularly required for the bend tubes used for superheater and reheater coils as a part of post-fabrication. In the absence of the same dissolved chromium carbide in the solution gets precipitated along the grain boundaries leaving a chromium depletion zone around the grains leading to a lowering of corrosion resistance of the metal.

Under the conditions of precipitated chromium carbides in the grain boundaries, the strength of the interior matrix region decreases and weakens the grain boundaries. The high yield strength as observed in the cracked tube coincides with the sensitized nature condition. Under these conditions, the stress arising out of the steam pressure concentrates in the grain boundary region, which substantially magnifies the strain's effect. The smaller volume of the comparatively weak grain boundaries leads to the accumulation of a higher magnitude of strain than the bulk level. This results in stress-induced precipitation cracking, particularly in strained bend tubes. In the absence of stabilization treatment during post-fabrication, and exposure to metal temperatures of 510 to 790 °C, the possibility of the formation of chromium carbides becomes imminent from the solution in SS347H and the same has been observed in the present case, although it has served for only 2 years in service.

Thus, the cause for the failure was attributed to the stress-induced carbide precipitation due to improper stabilization treatment.

Acknowledgements

The authors acknowledge Central Power Research Institute for the support extended in carrying out the investigation.

References

- [1] Central Electricity Authority, "Review of performance of Thermal Power Station, 2017-18," 2020.
- [2] M. J. Esmacher and M. J. Esmacher, "Stress Corrosion Cracking of Stainless Steel Components in Steam Service." [Online]. Available: <https://www.researchgate.net/publication/254544963>
- [3] R. Parrott and H. Pitts, "Chloride stress corrosion cracking in austenitic stainless steel (RR902)," 2011. [Online]. Available: <https://www.hse.gov.uk/research/rrpdf/rr902.pdf>
- [4] R. Saluja and D. K. . Moeed, "Emphasis of Embrittlement Characteristics in 304L and 316L Austenitic Stainless Steel," *IOSR J. Mech. Civ. Eng.*, vol. 11, no. 6, pp. 04–10, 2014, doi: 10.9790/1684-11650410.
- [5] Q. Zhou, S. Ping, X. Meng, R. Wang, and Y. Gao, "Precipitation Kinetics of M23C6 Carbides in the Super304H Austenitic Heat-Resistant Steel," *J. Mater. Eng. Perform.*, vol. 26, no. 12, pp. 6130–6139, Dec. 2017, doi: 10.1007/s11665-017-2982-2.
- [6] M. Schütze and W. J. Quadackers, Novel approaches to improving high-temperature corrosion resistance. 2008. doi: 10.1533/9781845694470.
- [7] A. S. Lima, A. M. Nascimento, D. De Engenharia, and D. De Engenharia, "Sensitization evaluation of the austenitic stainless steel AISI 304L, 316L, 321 and 347," vol. 0, pp. 139–144, 2005.
- [8] M. Ghalambaz, M. Abdollahi, A. Eslami, and A. Bahrami, "A case study on failure of AISI 347H stabilized stainless steel pipe in a petrochemical plant," *Case Stud. Eng. Fail. Anal.*, vol. 9, no. May, pp. 52–62, Oct. 2017, doi: 10.1016/j.csefa.2017.07.001.
- [9] J. Swaminathan, R. Singh, M. K. Gunjan, and B. Mahato, "Sensitization induced stress corrosion failure of AISI 347 stainless steel fractionator furnace tubes,"

Eng. Fail. Anal., vol. 18, no. 8, pp. 2211–2221, 2011, doi: 10.1016/j.engfailanal.2011.07.015.

[10]Z. Zheng, J. Zhang, X. Sun, J. Zhang, and H. He, “Failure analysis of the TP347H austenitic stainless steel tube of boiler reheater in a coal-fired power plant,” Eng. Fail. Anal., p. 105154, 2020, doi: 10.1016/j.engfailanal.2020.105154.

[11]A. Abou-Elazm, R. Abdel-Karim, I. Elmahallawi, and R. Rashad, “Correlation between the degree of

sensitization and stress corrosion cracking susceptibility of type 304H stainless steel,” Corros. Sci., vol. 51, no. 2, pp. 203–208, Feb. 2009, doi: 10.1016/j.corsci.2008.10.015.

[12]F. Stainless et al., “Standard Specification for Chromium and Chromium-Nickel Stainless Steel Plate, Sheet, and Strip for Pressure Vessels and General,” pp. 1–12, doi: 10.1520/A0240.